

Cite this: *Dalton Trans.*, 2021, **50**,
3717

Controlled di-lithiation enabled synthesis of phosphine-sulfonamide ligands and implications in ethylene oligomerization†‡

Nilesh R. Mote,^{a,b} Shahaji R. Gaikwad,^{a,b} Kishor V. Khopade,^{a,b}
Rajesh G. Gonnade ^c and Samir H. Chikkali ^{*a,b}

Catalyst design for ethylene oligomerization has attracted significant interest. Herein, we report the synthesis of phosphine-sulfonamide-derived palladium complexes and examine their performance in ethylene oligomerization. Arresting a dilithiation intermediate of *N*-(2-bromophenyl)-4-methylbenzenesulfonamide (**1**) at $-84\text{ }^{\circ}\text{C}$ selectively produced *N*-(2-(bis(2-methoxyphenyl)phosphanyl)phenyl)-4-methylbenzenesulfonamide (**L1A**). However, the same reaction at $-41\text{ }^{\circ}\text{C}$ delivered a different ligand; 2-(bis(2-methoxyphenyl)phosphanyl)-4-methyl-*N*-phenylbenzenesulfonamide (**L2A**). The generality of our strategy has been demonstrated by preparing *N*-(2-(diphenylphosphanyl)phenyl)-4-methylbenzenesulfonamide (**L1B**) and 2-(diphenylphosphanyl)-4-methyl-*N*-phenylbenzenesulfonamide (**L2B**). Subsequently, **L1A** and **L1B** were treated with a palladium precursor to yield 5-membered complexes **C1** and **C2**, respectively. In contrast, **L2A** upon treatment with palladium produced a 6-membered metal complex **C3**. Thus, a small library of 7 palladium complexes (**C1–C7**) were synthesized by varying the donor moiety (pyridine, DMSO, and acetonitrile). The identity of palladium complexes was unambiguously ascertained using a combination of spectroscopic and analytical methods, including single-crystal X-ray diffraction. The performance of the complexes **C1–C7** was investigated in ethylene oligomerization and almost all of them were found to be active. The resultant ethylene oligomers were characterized using ^1H and ^{13}C NMR, MALDI-ToF-MS, and GPC. Detailed screening of reaction parameters revealed $100\text{ }^{\circ}\text{C}$ and 40 bars ethylene to be optimal conditions. Complex **C5** outperformed other complexes and produced ethylene oligomers with a molecular weight of $1000\text{--}1900\text{ g mol}^{-1}$.

Received 11th January 2021,
Accepted 4th February 2021

DOI: 10.1039/d1dt00093d

rsc.li/dalton

Introduction

Metal catalyzed insertion polymerization of ethylene is known for seven decades and has revolutionized the polymer industry.^{1,2} The insertion polymerization can be tailored to obtain high to ultrahigh molecular weight polyethylene (PE), highly branched PE, functional PE, PE with renewable monomers, etc.^{3–6} Ligand steric and electronic parameters play a crucial role and enable outstanding performance.⁷

Furthermore, the method can be customized to produce dimers, trimers, tetramers, oligomers, and polymers.^{8,9} These resultant products tremendously influence our daily life and are being used as chemical intermediates, surfactants, and thermoplastics.^{10,11} Medium-chain length intermediates (*ca.* C12 and above) are termed oligomers and are being commercially produced over half a century.¹² Although several commercial processes are known to produce ethylene oligomers [like the Shell Higher Olefin Process (SHOP)], the foundation of these technologies appears to be the catalyst structure.^{13–17} Therefore, catalyst design for ethylene oligomerization to higher olefins has attracted significant interest from academia as well as industry.^{18–21} Although different metals have been tested in ethylene oligomerization, the 1st-row transition metals such as Cr, Fe, Co, and Ni appear to be the most investigated metals.^{9,22–24} Recent trends reveal that judiciously tailored Pd-complexes can catalyze ethylene oligomerization.^{25,26} For example, specific phosphine-sulfonate-derived palladium complexes are known to produce ethylene oligomers.^{27–30} Thus, few catalysts have been reported for ethylene oligomeri-

^aPolyolefin Laboratory, Polymer Science and Engineering Division, CSIR-National Chemical Laboratory, Dr. Homi Bhabha Road, Pune-411008, India.

E-mail: s.chikkali@ncl.res.in

^bAcademy of Scientific and Innovative Research (AcSIR), Anusandhan Bhawan, 2 Rafi Marg, New Delhi-110001, India

^cCenter for Materials Characterization, CSIR-National Chemical Laboratory, Dr Homi Bhabha Road, Pune-411008, India

†Dedicated to Dr Swaminathan Sivaram on the occasion of his 75th birthday.

‡Electronic supplementary information (ESI) available. CCDC 1977110–1977114. For ESI and crystallographic data in CIF or other electronic format see DOI: 10.1039/d1dt00093d

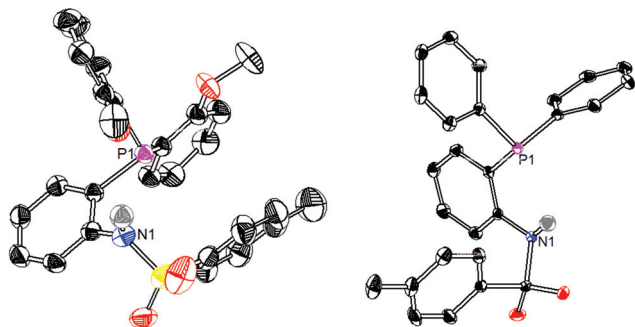


Fig. 1 Molecular structure of ligands (L1A) (left) and (L1B) (right); solvent molecules and H-atoms (except N-H) are omitted for clarity; thermal ellipsoids are drawn at the 50% probability level.

zation and Chart 1 (top) depicts recent phosphine-sulfonamide derived catalytic systems.

Brookhart and coworkers investigated the performance of phosphine-sulfonamide-derived nickel complex **A** (Chart 1). The neutral nickel complex catalyzed ethylene oligomerization and a degree of polymerization between 10 and 35 was reported.³¹ Phosphine-sulfonamide ligated Pd complexes of type **B** (Chart 1) have been recently reported by Chen and coworkers. These **B** type complexes were active in ethylene dimerization and trimerization. Enhanced activity was observed in the presence of Lewis acids such as $B(C_6F_5)_3$.³² In 2015, Mecking and co-workers reported the phosphine-sulfonamide ligands capable of forming P–O (**C**) and P–N (**D**) chelate with palladium (Chart 1).³³ The cationic complexes exhibited high catalytic activities for ethylene dimerization, yielding butenes with a high selectivity of up to 97.7%, while the neutral complexes displayed low activity. In 2019, Nozaki and co-workers reported a carbene-sulfonamide (Chart 1, **E**) ligand framework and prepared palladium complexes.³⁴ The Pd-complexes catalyzed ethylene oligomerization and ethylene/methyl acrylate co-oligomerization. Inspired by the above investigations, we

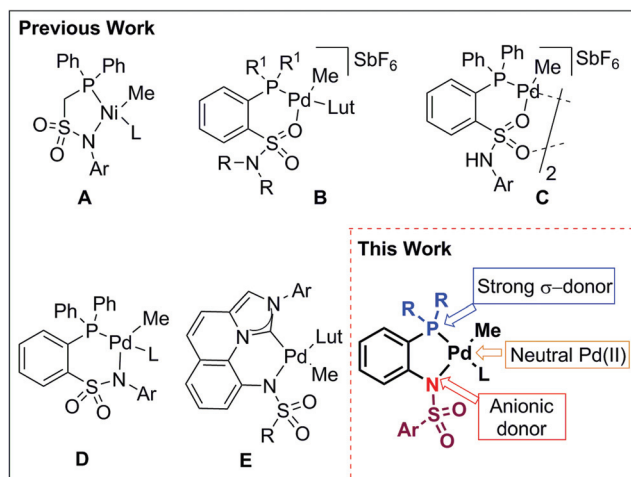


Chart 1 Phosphine-sulfonamide ligated metal complexes in ethylene oligomerization (A–E) and our approach.

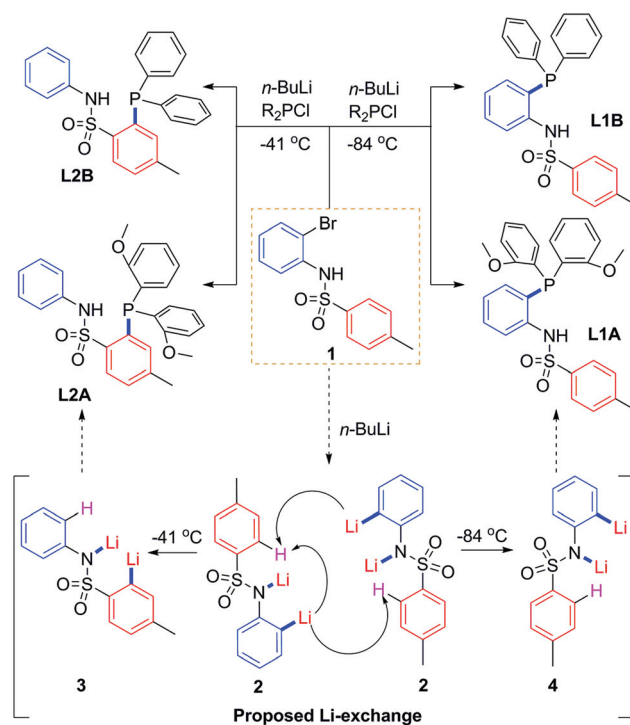
anticipated that the sulfonamide ligand with a pendent tosyl (external electron-withdrawing $-SO_2$) moiety would coordinate to palladium and might initiate ethylene oligomerization.

Herein, we report the controlled di-lithiation enabled synthesis of four phosphine-sulfonamide ligands, a small library of seven palladium complexes, and the behaviour of these complexes in ethylene oligomerization.

Results and discussion

Ligand synthesis

The precursor **1** [*N*-(2-bromophenyl)-4-methylbenzenesulfonamide] was prepared in 81% isolated yield by modifying the literature protocol.^{35,36} Compound **1** (0.5 g, 1.53 mmol) was treated with ~2 equivalents of *n*-BuLi (2 M solution, 1.51 mL, 3.03 mmol) at $-41^\circ C$ and chlorobis(2-methoxyphenyl)phosphane (0.43 g, 1.53 mmol) was added. A ^{31}P NMR spectrum of the reaction mixture displayed single resonance at -30.0 ppm and subsequent detailed analysis revealed the unexpected formation of 2-(bis(2-methoxyphenyl)phosphanyl)-4-methyl-*N*-phenylbenzenesulfonamide (**L2A**), instead of the anticipated product *N*-(2-(bis(2-methoxyphenyl)phosphanyl)phenyl)-4-methylbenzenesulfonamide (**L1A**) (Scheme 1). The existence of the ligand (**L2A**) was unambiguously confirmed by ^{31}P , 1H , 1-2D NMR, and electrospray ionization mass spectrometry (ESI-MS) (Fig. S6–S9[†]). The NMR assignments and mass spectroscopy data were found to match with literature reports on similar phosphine sulfonamide ligands.^{36–38} It is proposed that com-



Scheme 1 Controlled di-lithiation of **1** to produce phosphine sulfonamide ligands **L1A** and **L2A**. Subsequent scope to **L1B** and **L2B**.

compound **1** after lithiation generates intermediate **2**, which undergoes inter- or intra-molecular lithium exchange (as shown in Scheme 1) to produce species **3** *in situ*. It is most likely that the formation of **L2A** proceeds *via* this *in situ* generated species **3**. A paradigm shift could be achieved if the unstable di-lithiated intermediate **2** could be selectively formed and if the lithium exchange is arrested. In our attempts to address this bottleneck, we performed di-lithiation of *N*-(2-bromophenyl)-4-methylbenzenesulfonamide (**1**) with 2 equivalents of *n*-BuLi at different temperatures and time intervals. Our optimization disclosed that di-lithiation of **1** at $-84\text{ }^{\circ}\text{C}$ for 30 minutes followed by the addition of chlorobis(2-methoxyphenyl)phosphane (An_2PCl) at $-84\text{ }^{\circ}\text{C}$ selectively produces **L1A**. Subsequent acidic workup and purification delivered the desired phosphine ligand (**L1A**) in 85% isolated yield (Scheme 1).

The appearance of a single ^{31}P NMR resonance at -47.4 ppm clearly indicated the formation of **L1A**. The identity of **L1A** was unambiguously established using a combination of spectroscopic and analytical methods (Fig. S10–S15 \ddagger). Electrospray ionization mass spectrometric analysis of **L1A** revealed a molecular ion peak at $m/z = 492.1393$ [**L1A** + H] $^+$. Crystals suitable for X-ray diffraction were obtained by layering a DCM solution of **L1A** with hexane and the layered Schlenk was stored at $0\text{ }^{\circ}\text{C}$. Ligand **L1A** crystallizes in the triclinic unit cell in the P_1 space group. The molecular structure of **L1A** clearly shows the phosphine is covalently bonded *ortho* to sulfonamide (Fig. 1, left).

Thus, di-lithiation of **1** at $-41\text{ }^{\circ}\text{C}$ produces **L2A** *via* intermediate **3**, while the reaction at $-84\text{ }^{\circ}\text{C}$ selectively delivers **L1A**. The controlled lithiation strategy provides access to two ligands starting from the same precursor. Such a strategy is highly desirable and could be applied to generate a ligand library. To demonstrate the generality of this strategy, we set out to prepare two more ligands, **L1B** by performing the reaction at $-84\text{ }^{\circ}\text{C}$ and **L2B** at $-41\text{ }^{\circ}\text{C}$ (Scheme 1). In our attempts, 2 equivalents of *n*-BuLi (2 M, 3.06 mL, 6.13 mmol) were added to a THF solution of compound **1** at $-84\text{ }^{\circ}\text{C}$. After 30 minutes, chlorodiphenylphosphane (0.56 mL, 3.06 mmol) was added dropwise to the above reaction mixture at $-84\text{ }^{\circ}\text{C}$ and was stirred for 16 hours. Work up and purification produced **L1B** in 74% isolated yield. A ^{31}P NMR resonance at -26.4 ppm , ^1H , ^{13}C , and 1-2D NMR confirmed the formation of **L1B** (Fig. S16 \ddagger). The NMR findings were further corroborated by ESI-MS, which disclosed a molecular ion peak at $m/z = 432.1175\text{ Da}$ [**L1B** + H] $^+$ (Fig. S19 \ddagger). The existence of **L1B** was unambiguously ascertained from single-crystal X-ray diffraction analysis. Single crystal X-ray diffraction measurements revealed that **L1B** crystallizes in the triclinic space group and a P–C bond length of 1.83 \AA corresponding to covalent P–C bonds was observed (Fig. 1, right). As anticipated, when compound (**1**) was treated with *n*-BuLi and chlorodiphenylphosphane at $-41\text{ }^{\circ}\text{C}$, the formation of **L2B** was observed. The identity of **L2B** was established by 1-2D NMR spectroscopy and by using analytical methods. Thus, the controlled lithiation strategy provides access to 4 different ligands starting from one common precursor (compound **1**), in a single step, in very good to excellent isolated yields.

Synthesis of palladium complexes

The phosphine-sulfonamide ligands bear at least three donor atoms in their framework. Such ligands might display three types of coordination modes and Chart 2 depicts different chelation modes. Coordination through neutral phosphine and anionic amine will result in a five-membered ring (PN chelation) (Chart 2). While the negative charge can delocalize over the NS arm leading to a PSN complex, the formation of seven-membered palladium can be anticipated through PO chelation (Chart 2, PO).³⁹

The phosphine sulfonamide ligand (**L1A**) (0.100 g, 0.20 mmol) was treated with a palladium precursor $[(\text{TMEDA})\text{PdMe}_2]$ (0.051 g, 0.20 mmol) in pyridine (5 mL) (Scheme 2, top). The progress of the reaction was monitored by ^{31}P NMR, which revealed a single resonance at 26.3 ppm after 2 hours, indicating completion of the reaction. Co-evaporation and washing produced a solid compound in 91% isolated yield. The ^{31}P NMR spectrum of this residue (displayed a single peak at 26.3 ppm) suggested coordination of phosphine to palladium metal (Fig. S22 \ddagger). ^1H NMR revealed a characteristic resonance at 0.32 ppm, while the ^{13}C NMR disclosed a resonance at -2.7 ppm that can be assigned to the Pd–Me group in **C1** (Fig. S23 and S24 \ddagger). The above ^{31}P , ^1H , and ^{13}C NMR shifts closely match with literature reported similar palladium complexes.^{38,40} The NMR findings were corroborated by ESI-MS and a molecular ion peak was observed at $m/z = 691.0795$ [**C1** + H] $^+$ (Fig. S31 \ddagger). An unambiguous demon-

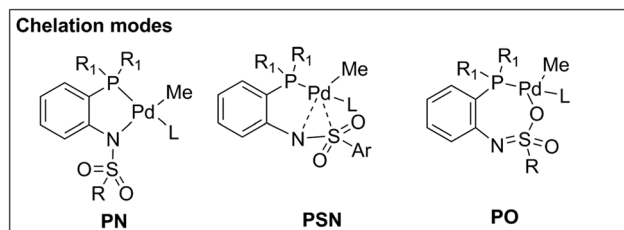
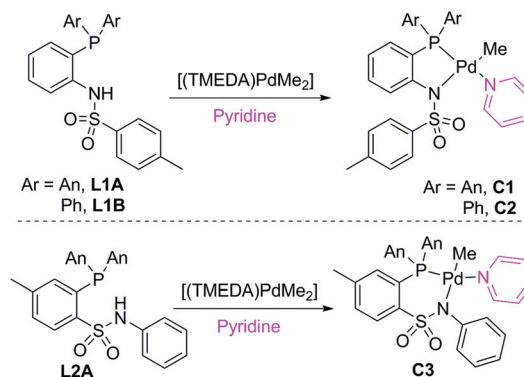


Chart 2 Possible coordination modes of the phosphine-sulfonamide ligand.



Scheme 2 Synthesis of palladium complexes **C1**, **C2** and **C3**.

stration of the coordination of **L1A** was revealed by single-crystal X-ray diffraction of **C1**. The molecular structure disclosed the formation of a 5-member ring and PN coordination to yield **C1**. Fig. 2 depicts the molecular structure of complex

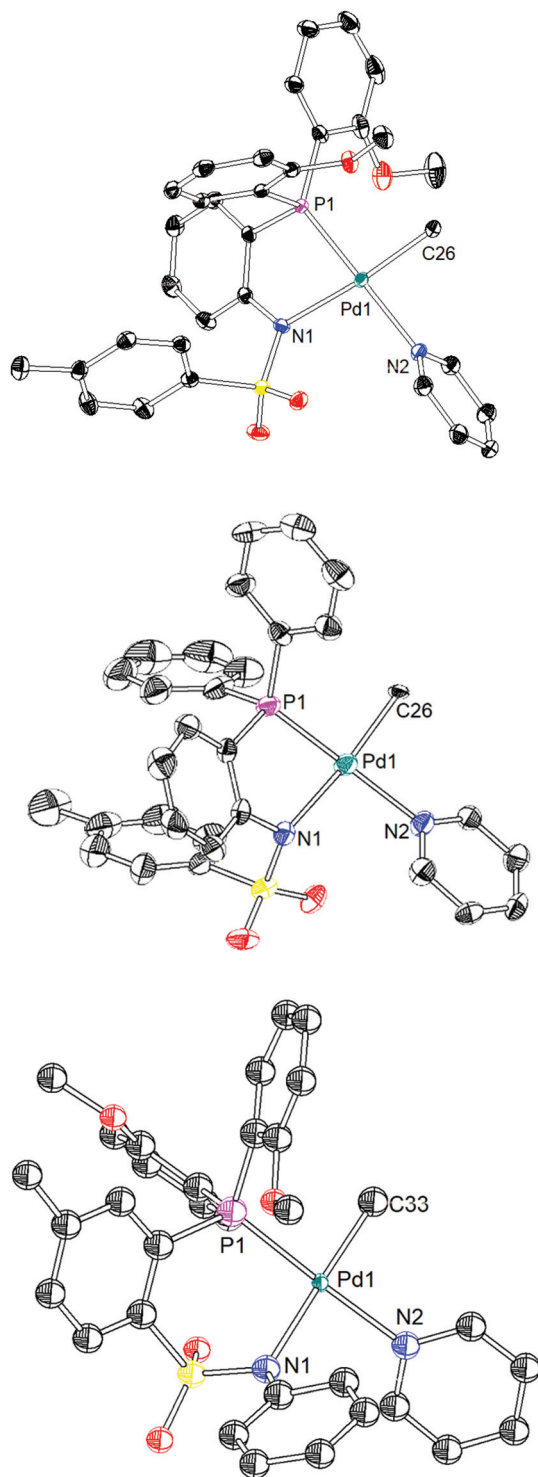


Fig. 2 Molecular structures of palladium complexes **C1** (top), **C2** (center), and **C3** (bottom); solvent molecules and H-atoms are omitted for clarity; thermal ellipsoids are drawn at the 50% probability level.

C1. Crystals of **C1** grew in the monoclinic unit cell in the $P\bar{1}$ space group. The crystal consists of a central palladium atom with a distorted square planar geometry and is surrounded by bis-chelating (**L1A**), a methyl group, and a coordinating pyridine molecule per formula unit. The P–Pd bond distance of 2.20 Å (Fig. 2, top) confirms the formation of a coordinate bond.⁴¹ The donor molecule pyridine revealed a Pd–N2 bond distance of 2.11 Å.⁴²

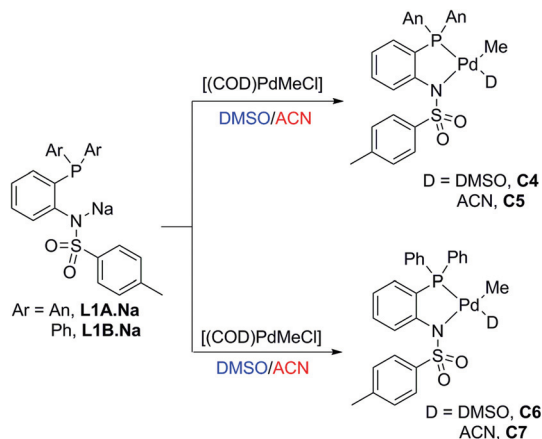
The pyridine is placed *trans* to phosphine while the sulfonamide nitrogen atom is *trans* to the methyl group. The methyl group on palladium and donor pyridine occupy *cis*-disposition ($C26-Pd1-N2 = 86.82^\circ$), which is a prerequisite for a metal complex to be active in insertion polymerization.⁴³

Along the same lines, phosphine sulfonamide ligand **L1B** was treated with a palladium precursor to produce palladium complex **C2** in 92% isolated yield. The ³¹P NMR spectrum revealed a single peak at 40.8 ppm, confirming the coordination of phosphine to palladium metal (Fig. S33[†]). While ¹H NMR displayed a characteristic resonance at 0.42 ppm, ¹³C NMR revealed a peak at –2.4 ppm, which can be assigned to the methyl group located on the palladium in **C2** (Fig. S34 and S35[†]).

The observed ESI-MS further supported the existence of **C2** and single-crystal X-ray diffraction unambiguously ascertained the formation of **C2**. **C2** crystallizes in a triclinic unit cell with two molecules of the complex per unit cell (Fig. 2, center). The central palladium shows a distorted square planar geometry and similar bonding arrangements to that of **C1**.

Among **L2A** and **L2B**, the coordination behavior of **L2A** was investigated. Thus, **L2A** produced complex **C3** in 92% isolated yield (Scheme 2, bottom). The existence of the complex **C3** was established using spectroscopic and analytical methods. ³¹P NMR shows a single peak at 22.8 ppm which suggests coordination of phosphine to palladium metal (Fig. S44[†]). ¹H NMR displayed a characteristic peak at 0.04 ppm for the Pd–Me group which suggests the formation of the desired Pd complex **C3** (Fig. S45[†]). The existence of **C3** was further authenticated by single-crystal X-ray diffraction analysis (Fig. 2, bottom). X-ray diffraction of **C3** revealed that the phosphine-sulfonamide ligand (**L2A**) coordinates to the Pd-center and forms a 6 membered ring, in contrast to 5 membered rings in **C1** and **C2** (Fig. 2, top). The metal-containing ring displays a P–Pd–N angle of $\sim 94^\circ$ which is larger than the P–Pd–N angle in **C1** and **C2**.

It is known in the literature that weakly coordinating donor groups such as DMSO or acetonitrile display better activity in ethylene insertion polymerization.^{44–47} Given the literature precedence and better performance of such donor groups, we set out to prepare complexes **C4**–**C7** (Scheme 3). The sodium salt of **L1A** and **L1B** was treated with [(COD)PdMeCl]/[(DMSO)PdMeCl]₂ to produce **C4**–**C7** in good to excellent yields. Treating sodium salt of ligand (**L1A**) (**L1A.Na**) with [(COD)PdMeCl] produces complex **C4** in good yield (66%) (Scheme 3, top). The existence of complex **C4** was established using 1-2D NMR and ESI-MS analysis. Furthermore, the existence of the complex **C4** was authenticated by the appearance of a pseudo-



Scheme 3 Synthesis of palladium complexes **C4**, **C5**, **C6**, and **C7**.

molecular ion peak at $m/z = 612.0586$ $[\text{M-DMSO} + \text{H}]^+$ (Fig. S55 \ddagger).

Similarly, metal complexes **C5**, **C6**, and **C7** were prepared in good to excellent yields by treating the ligand (**L1A/B**) with the palladium precursor (Scheme 3). The identity of **C5–C7** was established using a combination of 1-2D NMR spectroscopy, ESI-MS, and analytical methods. A characteristic down-field shifted ^{31}P NMR, the appearance of Pd–Me protons between 0.04 and 0.55, corresponding up-field shifted ^{13}C NMR resonances, and ESI-MS unambiguously authenticated the formation of complexes **C5–C7** (Fig. S56–S71 \ddagger).

C1–C7 catalyzed ethylene oligomerization

Neutral palladium complexes such as **C1–C7** can catalyze ethylene oligomerization without the aid of any co-catalyst. Performance of palladium complexes **C1–C7** in ethylene oligomerization was examined and Table 1 reports the most important results. The pyridine coordinated palladium catalyst **C1** was found to produce a trace amount of highly viscous liquid at 80 °C (Table 1, entry 1). However, increasing the temperature to 90 °C produced 15–19 mg of semi-solid material (Table 1, entries 2 and 3). A similar quantity of semi-solid material was produced by catalyst **C2** at 80–90 °C (Table 1, entries 4–6). The 6-membered palladium complex **C3** produced a trace amount of material at 90 °C. But increasing the polymerization temperature to 100 °C and addition of Lewis acid ($\text{B}(\text{C}_6\text{F}_5)_3$) failed to produce an observable amount of material (Table 1, entry 8). The reduced activity of **C1–C3** can be ascribed to the strong coordination of pyridine to the palladium center. It is well documented in the literature that the pyridine coordinated palladium catalysts often display poor activity.

Literature reports suggest that substituting pyridine with weakly coordinating donors such as DMSO or acetonitrile might help in increasing the catalytic activity. Thus, a DMSO coordinated complex **C4** was evaluated in the ethylene oligomerization reaction (Table 1, entries 9–11). Indeed, exposing **C4** to ethylene led to the production of an increased quantity (74 mg) of semi-solid material.

Table 1 **C1–C7** catalyzed ethylene oligomerization

Entry	Catalysts	Temp. (°C)	Press. (bar)	Yield (mg)	TOF (mol of OE per mol of Pd h ⁻¹)
1	C1	80	10	Trace	—
2	C1	90	10	15	8
3	C1	90	20	19	11
4	C2	80	10	Trace	—
5	C2	90	10	10	5
6	C2	90	20	15	—
7	C3	90	10	Trace	—
8 ^a	C3	100	40	NO	—
9	C4	80	20	60	34
10	C4	90	10	67	37
11	C4	90	20	74	42
12	C5	80	10	64	36
13	C5	90	10	101	57
14	C5	100	10	99	56
15	C5	100	20	104	58
16	C5	100	30	106	60
17	C5	100	40	141	80
18	C5	110	10	103	58
19	C5	110	20	106	60
20	C5	110	30	102	58
21	C5	110	40	99	56
22	C5	120	40	97	55
23 ^a	C5	100	40	111	63
24	C6	70	10	Trace	—
25	C6	80	10	17	9
26	C6	90	10	43	24
27	C7	80	10	39	22
28	C7	90	10	53	30
29 ^b	C5	90	10	97	29
30 ^c	C5	90	10	99	14

Reaction conditions: catalyst = 63 μmol in DCM (10 mL), toluene = 100 mL, ethylene = 10–40 bars, time = 1 h, OE = oligoethylene, NO = not observed, ND = not determined, the reported yield is after subtracting catalyst quantity from the final weight of solids/semi-solids, a = $\text{B}(\text{C}_6\text{F}_5)_3$ was used as an additive to activate the catalysts, b and c = oligomerization was performed for 2 h and 4 h respectively.

In contrast, the acetonitrile coordinated complex **C5** produced *ca.* 100 mg of semi-solid material under identical conditions (Table 1, entry 13). The labile coordination of acetonitrile in **C5** could be responsible for the increased activity. Motivated by the better performance of **C5**, detailed screening was conducted for this catalyst. The effect of ethylene pressure at 100 °C was evaluated. As evident from Table 1, entry 14–17, with increasing ethylene pressure the quantity of ethylene oligomers increased. At 100 °C and 40 bars ethylene pressure, nearly 140 mg of semisolid material was obtained (Table 1, entry 15). Detailed analysis of this material (Table 1, entry 15) revealed the presence of ethylene oligomers. A ^{13}C NMR disclosed a characteristic methylene repeat unit peak at 29.3 ppm (Fig. S73 \ddagger), flanked by other low-intensity signals between 10 and 37 ppm. These resonances can be ascribed to various (methyl, ethyl, propyl, butyl, *etc.*) branches on oligomeric ethylene.⁴⁸ The proton NMR revealed an absolute number average molecular weight of 1100 g mol^{-1} , and GPC measurements displayed a similar weight average molecular weight of 1100 g mol^{-1} . MALDI-ToF-MS analysis of the resultant material revealed a repeat unit mass of 28 Da (Fig. S87 and 88 \ddagger). Thus, complex **C5** produced highly branched ethylene oligomers.

While further increasing the polymerization temperature to 110 °C resulted in diminished polymer yield (Table 1, entries 18–21), increasing the polymerization temperature further to 120 °C proved futile (Table 1, entry 22). When the phenyl substituted complexes, C6 and C7, were evaluated, the formation of up to 53 mg of oligomeric semi-solid material was observed. Thus, complexes C1–C3 with pyridine ligation underperform and display very low or no activity. However, DMSO and acetonitrile coordinated complexes C4–C7 revealed better performance. Among these C4–C7, anisole-derived complexes C4 and C5 displayed better performance than their phenyl counterparts C6 and C7. Clearly, complex C5 with anisole substituents on the phosphine phosphorus and the ACN donor is a superior catalyst for ethylene oligomerization. Analysis of the resultant semi-solid material indicates formation of highly branched oligomers. Formation of branched oligomers suggests that C4–C7 are susceptible to insertion and fast β -hydride elimination. The microstructure analysis of oligoethylenes displayed ^{13}C NMR resonances at 10.9, 14.11, 19.7, and 27.0 ppm. Based on literature precedence, these peaks can be ascribed to various methyl, ethyl, propyl and butyl branches.¹⁹ Thus, the observed branching could be a result of β -hydride elimination (after a few ethylene insertions) and reinsertion of the eliminated olefin. The down-field shifted ^{13}C NMR resonances at 114.0 and 139.2 (Fig. S73 \ddagger) can be assigned to chain-end double bonds.⁴⁹ Although C5 is the best among C1–C7, better catalysts for ethylene oligomerization have been reported in the literature.^{16,19,20,26}

Conclusions

In summary, arresting di-lithiation of *N*-(2-bromophenyl)-4-methylbenzenesulfonamide (**1**) provided access to two different ligands. Controlled lithiation of **1** at –84 °C selectively yields ligand *N*-(2-(bis(2-methoxyphenyl)phosphanyl)phenyl)-4-methylbenzenesulfonamide (**L1A**), while the same reaction at –41 °C enabled access to 2-(bis(2-methoxyphenyl)phosphanyl)-4-methyl-*N*-phenylbenzenesulfonamide (**L2A**). Subsequently, ligands *N*-(2-(diphenylphosphanyl)phenyl)-4-methylbenzenesulfonamide (**L1B**) and 2-(diphenylphosphanyl)-4-methyl-*N*-phenylbenzenesulfonamide (**L2B**) were prepared in excellent yields to demonstrate the generality of our synthetic protocol. Exposing **L1A** and **L1B** to [(TMEDA)PdMe₂] selectively produced 5-membered palladium complexes C1 and C2 respectively. In contrast, treating the ligand (**L2A**) with a palladium precursor generated a 6-membered palladium complex C3. The identity of C1–C3 was unambiguously established using 1-2D NMR, analytical methods, and single-crystal X-ray diffraction. Similarly, when sodium salts of **L1A** and **L1B** were treated with [(COD)PdMeCl] in either DMSO or acetonitrile, the corresponding palladium complexes C4–C7 were produced in good to excellent yields. Thus, a small library of seven complexes were generated starting from a single ligand precursor and the performance of C1–C7 was tested in ethylene oligomerization.

The pyridine-coordinated complexes C1–C3 were found to be active; however, these complexes revealed a very poor yield in the ethylene oligomerization reaction. The poor performance can be ascribed to the stronger coordination of pyridine (to palladium), without leaving any scope for ethylene coordination. While weakly coordinating DMSO complex C4 revealed a better performance with 74 mg of ethylene oligomers, the acetonitrile-coordinated complex C5 revealed an improved performance with ca. 100 mg of ethylene oligomers. Optimization of reaction parameters using C5 indicated 100 °C at 40 bars as an optimal reaction condition. Nearly 140 mg of ethylene oligomer with a molecular weight of 1100 g mol^{–1} was produced under these optimal conditions.

Conflicts of interest

There are no conflicts to declare.

Acknowledgements

We are indebted to DST-SERB (EMR/2016/005120), CSIR-NCL (HCP0011), India, and AvH Foundation Bonn, Germany for financial support.

Notes and references

- 1 E. Y.-X. Chen and T. J. Marks, *Chem. Rev.*, 2000, **100**, 1391.
- 2 J. Chen, Y. Gao and T. J. Marks, *Chem. Rev.*, 2020, **59**, 14726.
- 3 M. Chen and C. Chen, *Angew. Chem.*, 2019, **59**, 1206.
- 4 T. Liang, S. B. Goudari and C. Chen, *Nat. Commun.*, 2020, **11**, 372.
- 5 K. Patel, S. Sivaram and S. H. Chikkali, *Prog. Polym. Sci.*, 2020, **109**, 101290/1-30.
- 6 Y. Na and C. Chen, *Angew. Chem.*, 2020, **59**, 7953.
- 7 Q. Muhammad, C. Tan and C. Chen, *Sci. Bull.*, 2020, **65**, 300.
- 8 D. S. McGuinness, *Chem. Rev.*, 2011, **111**, 2321.
- 9 C. Bariashir, C. Huang, G. A. Solan and W.-H. Sun, *Coord. Chem. Rev.*, 2019, **385**, 208.
- 10 M. C. Baier, M. A. Zuideveld and S. Mecking, *Angew. Chem., Int. Ed.*, 2014, **53**, 9722.
- 11 S. Chikkali, *Resonance*, 2017, **22**, 1039.
- 12 O. L. Sydora, *Organometallics*, 2019, **38**, 997.
- 13 W. Keim, *Angew. Chem., Int. Ed.*, 2013, **52**, 12492.
- 14 D. S. McGuinness, P. Wasserscheid, W. Keim, D. Morgan, J. T. Dixon, A. Bollmann, H. Maumela, F. Hess and U. Englert, *J. Am. Chem. Soc.*, 2003, **125**, 5272.
- 15 A. Boudier, P.-A. Breuil, L. Magna, H. Olivier-Bourbigou and P. Braunstein, *Chem. Commun.*, 2014, **50**, 1398.
- 16 D. F. Wass, *Dalton Trans.*, 2007, 816.
- 17 J. T. Dixon, M. J. Green, F. M. Hess and D. H. Morgan, *J. Organomet. Chem.*, 2004, **689**, 3641.

- 18 Y. Gao, J. Chen, Y. Wang, D. B. Pickens, A. Motta, Q. J. Wang, Y.-W. Chung, T. L. Lohr and T. J. Marks, *Nat. Catal.*, 2019, **2**, 236.
- 19 T. Wiedemann, G. Voit, A. Tchernook, P. Roesle, I. Göttker-Schnetmann and S. Mecking, *J. Am. Chem. Soc.*, 2014, **136**, 2078.
- 20 D. J. Arriola, B. C. Bailey, J. Klosin, Z. Lysenko, G. R. Roof and A. J. Smith, Dow Global Technologies LLC., *Patent*, WO2014/209927A1, 2014.
- 21 G. J. P. Britovsek, R. Malinowski, D. S. McGuinness, J. D. Nobbs, A. K. Tomov, A. W. Wadsley and C. T. Young, *ACS Catal.*, 2015, **5**, 6922.
- 22 Z. Wang, G. A. Solan, W. Zhang and W.-H. Sun, *Coord. Chem. Rev.*, 2018, **363**, 92.
- 23 W. Zhang, H.-W. Sun and C. Redshaw, *Dalton Trans.*, 2013, **42**, 8988.
- 24 A. Finiels, F. Fajula and V. Hulea, *Catal. Sci. Technol.*, 2014, **4**, 2412.
- 25 D. Bézier, O. Daugulis and M. Brookhart, *Organometallics*, 2017, **36**, 443.
- 26 N. D. Contrella and R. F. Jordan, *Organometallics*, 2014, **33**, 7199.
- 27 Z. Cai, Z. Shen, X. Zhou and R. F. Jordan, *ACS Catal.*, 2012, **2**, 1187.
- 28 N. D. Contrella, J. R. Sampson and R. F. Jordan, *Organometallics*, 2014, **33**, 3546.
- 29 T. M. J. Anselment, C. Wichmann, C. E. Anderson, E. Herdtweck and B. Rieger, *Organometallics*, 2011, **30**, 6602.
- 30 A large number of phosphine-sulfonate-derived palladium complexes are highly efficient catalysts for ethylene-functional olefin copolymerization. For selected reviews on this topic, see: A. Nakamura, T. M. J. Anselment, J. Claverie, B. Goodall, R. F. Jordan, S. Mecking, B. Rieger, A. Sen, P. W. N. M. van Leeuwen and K. Nozaki, *Acc. Chem. Res.*, 2013, **46**, 1438.
- 31 M. J. Rachita, R. L. Huff, J. L. Bennett and M. Brookhart, *J. Polym. Sci., Part A: Polym. Chem.*, 2000, **38**, 4627.
- 32 Y. Zhang, Y. Cao, X. Leng, C. Chen and Z. Huang, *Organometallics*, 2014, **33**, 3738.
- 33 Z. Jian, L. Falivene, P. Wucher, P. Roesle, L. Caporaso, L. Cavallo, I. Göttker-Schnetmann and S. Mecking, *Chem. – Eur. J.*, 2015, **21**, 2062.
- 34 W. Tao, X. Wang, S. Ito and K. Nozaki, *J. Polym. Sci., Part A: Polym. Chem.*, 2019, **57**, 474.
- 35 See ESI for experimental details.‡
- 36 Ref. 31 reports the synthesis.
- 37 Please note that in ref. 33, Mecking and co-workers employed *N*-benzenesulfonamide as the precursor, while, we started with *N*-(2-bromophenyl)-4-methylbenzenesulfonamide and ended up getting similar ligand.
- 38 T. Kochi, K. Yoshimura and K. Nozaki, *Dalton Trans.*, 2006, 25.
- 39 For PSN coordination modes see: C. W. Tate, A. DeMellow, A. D. Gee, S. Kealey, R. Vilar, A. J. P. White and N. J. Long, *Dalton Trans.*, 2012, **41**, 83.
- 40 S. Luo, J. Vela, G. R. Lief and R. F. Jordan, *J. Am. Chem. Soc.*, 2007, **129**, 8946.
- 41 A P–Pd coordinate bond is reported earlier, see: S. R. Gaikwad, S. S. Deshmukh, R. G. Gonnade, P. R. Rajamohan and S. H. Chikkali, *ACS Macro Lett.*, 2015, **4**, 933.
- 42 For Pd-Pyridine coordination and bond distances see: S. S. Deshmukh, S. R. Gaikwad, R. J. Gonnade, S. P. Pandole and S. H. Chikkali, *Chem. – Asian J.*, 2020, **15**, 398.
- 43 Insertion intermediates have been trapped to signify the disposition of donor group and the olefin insertion species have been crystallized, see: S. R. Gaikwad, S. S. Deshmukh, V. S. Koshti, S. Poddar, R. G. Gonnade, P. R. Rajamohan and S. H. Chikkali, *Macromolecules*, 2017, **50**, 5748.
- 44 D. Guironnet, P. Roesle, T. Rünzi, I. Göttker-Schnetmann and S. Mecking, *J. Am. Chem. Soc.*, 2009, **131**, 422.
- 45 A. Nakamura, S. Ito and K. Nozaki, *Chem. Rev.*, 2009, **109**, 5215.
- 46 S. S. Deshmukh, S. R. Gaikwad, N. R. Mote, M. Manod, R. G. Gonnade and S. H. Chikkali, *ACS Omega*, 2019, **4**, 9502.
- 47 N. R. Mote, K. Patel, D. R. Shinde, S. R. Gaikwad, V. S. Koshti, R. G. Gonnade and S. H. Chikkali, *Inorg. Chem.*, 2017, **56**, 12448.
- 48 Z. Guan, P. M. Cotts, E. F. McCord and S. J. McLain, *Science*, 1999, **283**, 2059.
- 49 L. Pei, F. Liu, H. Liao, J. Gao, L. Zhong, H. Gao and Q. Wu, *ACS Catal.*, 2018, **8**, 1104.